

# **EOS AQUA AMSR-E SEA ICE VALIDATION PLAN**

**24 January 2003**

## TABLE OF CONTENTS

### PREFACE

### PART I ARCTIC SEA ICE VALIDATION PLAN

<b>1</b>	<b>INTRODUCTION</b> .....	6
1.1	<b>AMSR-E Sea Ice Product Validation</b> .....	6
1.2	<b>Satellite Measurements of Coastal Polynyas and Surface Heat and Moisture Flux Measurements</b> .....	6
<b>2</b>	<b>OBJECTIVES</b> .....	8
2.1	<b>Sea Ice Validation Objectives</b> .....	8
2.1.1	Validation Criteria.....	8
2.1.2	Accuracy Goal.....	8
2.2	<b>Arctic Coastal Polynya Objectives</b> .....	10
2.2.1	Satellite Measurement of Coastal Polynyas.....	10
2.2.2	Surface Heat and Moisture Flux Measurements.....	10
<b>3</b>	<b>VALIDATION DATA SOURCES</b> .....	11
3.1	<b>Satellite</b> .....	11
3.1.1	Passive and Active Microwave.....	11
3.1.2	Visible/IR.....	11
3.2	<b>Aircraft</b> .....	12
3.2.1	NASA WFF P-3B.....	12
3.2.2	NSF Aerosonde UAV.....	14
3.3	<b>Surface</b> .....	16
3.3.1	Barrow.....	16
3.3.2	Navy Ice Camp.....	18
3.3.3	Nome.....	19
3.3.4	Other Field Programs of Opportunity.....	19
<b>4</b>	<b>APPROACH</b> .....	19
4.1	<b>Sea Ice Validation Approach</b> .....	19
4.1.1	Beaufort and Northern Bering Seas (March 2003).....	22
4.1.2	Bering and Chukchi Seas (Feb/Mar 2005).....	23
4.2	<b>Polynya Surface Flux Measurement Approach</b> .....	24
4.3	<b>Arctic Flight Operations</b> .....	24
<b>5</b>	<b>MODELING AND SENSITIVITY ANALYSES</b> .....	28
<b>6</b>	<b>PROGRAM MANAGEMENT AND COORDINATION</b> .....	28
<b>7</b>	<b>DATA MANAGEMENT AND DATA AVAILABILITY</b> .....	29
<b>8</b>	<b>ARCTIC CAMPAIGN SCHEDULE</b> .....	30
<b>9</b>	<b>REFERENCES</b> .....	30

## **PART II     ANTARCTIC SEA ICE VALIDATION PLAN**

### **1. Introduction**

### **2. Scientific Justification**

- 2.1 Algorithm Validation Objectives
- 2.2 Process and Climate Change Studies Objectives
- 2.3 Coordination with Other NASA Programs

### **3. Algorithm Validation Issues**

- 3.1 Ice Concentration
- 3.2 Surface Ice Temperature
- 3.3 Snow Thickness

### **4. Process and Climate Change Study Issues**

- 4.1 Thin ice/polynya Studies
- 4.2 Surface heat and humidity fluxes
- 4.3 Thickness, Topography and Drag Coefficients
- 4.4 Ice Edge/Ice extent Studies

### **5. Methods and Techniques**

- 5.1 Coordinated Aircraft Programs
  - 5.1.1 Winter Flight Program (August-September 2003)
  - 5.1.2 Spring/Summer Flight Program (October-November 2004)
- 5.2 High Resolution Satellite
- 5.3 Ship, Buoy, and other In-Situ Data
- 5.4 Radiative Transfer Modeling of the Atmosphere and Sea Ice

### **6. Validation Schedule**

### **7. Data Management and Archival**

### **8. Personnel**

### **9. References**

## PREFACE

The Advanced Microwave Scanning Radiometer for EOS (AMSR-E) was successfully launched on NASA's EOS Aqua spacecraft on May 4, 2002. With the launch of this state-of-the-art radiometer, designed and built by NASDA of Japan, the sea ice research community will have available passive microwave sea ice products at a higher spatial resolution and a greater spectral range than previously possible. To make these sea ice products a useful research tool, a comprehensive AMSR-E sea ice validation program has been developed and will be implemented starting in 2003. This document outlines the program which consists of three main components: sea ice product comparisons using coincident high-resolution spaceborne data, comparisons using aircraft and surface data, and sensitivity, error, and model analyses. This validation plan outlines each component and the methods to be used to meet the validation objectives.

The two polar regions of the Earth, the Arctic and the Antarctic, have large sea ice covers that differ markedly in their physical, chemical, and electrical properties because of the very different environmental factors at work during and after sea ice formation. For these reasons and for the reason that the field campaign logistics are quite different in these two regions, this document is divided into two parts. The first part of this document covers the Arctic sea ice validation campaign, whereas the second part covers the Antarctic campaign. Both campaigns have similar validation objectives and each consists of the three main components noted above.

All the AMSR-E sea ice standard products are level 3 products and include sea ice concentration, sea ice temperature, and snow depth on sea ice. These products together with AMSR-E calibrated brightness temperatures (TBs) will be mapped to the same polar stereographic projection used for SSM/I data to provide the research community consistency and continuity with the existing 23-year Nimbus 7 SMMR and DMSP SSM/I sea ice concentration products archived on the SSM/I grid. The grid resolutions are as follows: (a) TBs for all AMSR-E channels: 25-km, (b) TBs for the 18, 23, 36, and 89 GHz channels: 12.5-km, (c) TBs for the 89 GHz channels: 6.25-km, (d) Sea ice concentration: 12.5-km, 25-km, (e) Sea ice temperature: 25-km, (f) Snow depth on sea ice: 12.5. All of the sea ice products will be validated at their respective grid resolutions.

The sea ice concentration products will be generated using three algorithms: the enhanced NASA Team (NT2) algorithm (Markus and Cavalieri, 2000; Comiso et al., 2003), the Bootstrap algorithm (BBA), and the AMSR Bootstrap Algorithm (ABA) (Comiso, and Zwally, 1997; Comiso et al., 2003). In the Arctic, the NT2 algorithm will provide the standard sea ice concentrations at both the 12.5 km and 25 km resolutions. In the Antarctic, the BBA and the ABA algorithms will provide the concentrations at the 12.5 km and 25 km resolutions, respectively. The ABA algorithm requires the 6 GHz data to reduce ice temperature effects and to generate ice temperature maps. Since the resolution of the 6 GHz is too coarse for a 12.5 km resolution retrieval, we use the BBA algorithm that makes use of the same sets of channels used in the Arctic version to generate the latter product. Differences between the algorithm ice concentration retrievals at their respective resolutions will also be provided for each hemisphere. The ice temperature will be produced from the ABA algorithm for both hemispheres and snow depth will be produced from the algorithm described by Markus and Cavalieri (1998) for both hemispheres, but excluding the Arctic perennial ice regions.

**PART I      ARCTIC SEA ICE VALIDATION PLAN**

D. J. Cavalieri, J. C. Comiso, E. Kim, and T. Markus  
Laboratory for Hydrospheric Processes  
NASA Goddard Space Flight Center  
Greenbelt, MD 20771

A. J. Gasiewski  
NOAA Environmental Technology Laboratory  
Boulder CO 80305

J. Heinrichs  
Dept. of Geosciences  
Fort Hays State University  
Hays, KS 67601

W. B. Krabill  
NASA  
Wallops Flight Facility  
Wallops Island, VA 23337

J. Maslanik and J. Stroeve  
University of Colorado  
Boulder, CO 80309

M. Sturm  
Cold Regions Research and Engineering Laboratory  
USA-CRREL-Alaska  
P.O. Box 35170  
Ft. Wainwright, AK 99703-0170

K. L. Thornhill and J. Barrick  
NASA Langley Research Center  
Hampton, VA 23665

B. Walter  
Northwest Research Associates  
Bellevue, WA 98009

## 1 INTRODUCTION

The Arctic NASA aircraft campaign integrates the requirements for obtaining the field data needed both for the validation of the standard AMSR-E sea ice products and for supporting ongoing studies of air-sea-ice interactions in Arctic coastal polynyas. This latter element falls within NASA's Cryospheric Sciences Program and has as its Earth Science Enterprise goal to understand how the Earth's climate system is changing.

### 1.1 AMSR-E Sea Ice Product Validation

In the Arctic, sea ice conditions vary considerably from region to region. The approach taken will be to focus on those regions and conditions that are known to give rise to the largest errors and the largest differences between the two sea ice concentration algorithms. From previous comparative studies potential difficulties with both of these algorithms have been identified. These include the influence of sea ice temperature variability on the ABA algorithm retrievals and the influence of atmospheric variability on the NT2 algorithm. Other problems common to both algorithms include ice concentration biases associated with unresolved ice or surface conditions. One example is the low concentration bias associated with the presence of new and young sea ice.

Our strategy will be to utilize a combination of spatially and temporally coincident surface, aircraft, and satellite observations to provide the requisite data needed to meet the validation objectives for the sea ice concentration products. The sea ice temperature and snow depth retrievals are considerably more difficult to validate. Our strategy for snow depth will be to employ both a specially designed airborne radar as well as surface-based snow depth measurements. Temperature validation will also depend in part on surface transects coordinated with aircraft overflights. The following sections will describe in detail the objectives and approach to be taken for the validation of each of these sea ice products.

### 1.2 Satellite Measurements of Coastal Polynyas and Surface Heat and Moisture Flux Measurements

Polynyas located over the continental shelves of the peripheral seas of the Arctic Ocean provide a mechanism for the growth of large amounts of ice in limited geographic areas. These areas are a source of relatively large amounts of salt that maintain the cold, halocline layer of the Arctic Ocean (Figure 1.1 from Aagaard et al., 1981). Although polynyas cover only 3-4% of the area of the Arctic, they control up to 50% of the ocean-to-atmosphere heat transfer in winter. Recurrent polynyas in the western Arctic form on the Canadian and Alaskan coasts from Banks Island to the Bering Strait and on the Siberian coast from the Bering Strait to the New Siberian Islands and have been the subject of both modeling (Björk, 1989; Winsor and Björk, 2000) and satellite observational studies (Cavalieri and Martin, 1994; Weingartner et al., 1998). The dense shelf water formed in these coastal polynyas depends on the ice production which in turn depends on the ocean to atmosphere heat flux. The observational studies cited above crudely estimate these fluxes over the coastal polynya open water areas by using a combination of satellite-observed open water areas and either weather station or surface weather analyses data. The sensible heat flux varies by three orders of magnitude as the polynya opens and closes. During winter

and early spring large air-sea temperature differences can result in heat fluxes of 500-1000 W/m<sup>2</sup> (Walter, 1989).

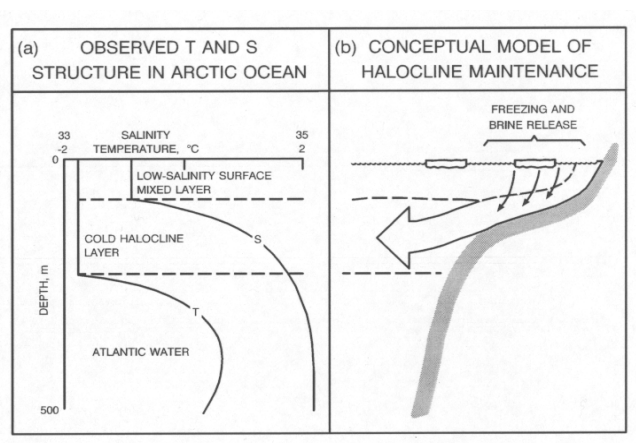


**Figure 1.1** Schematic diagram illustrating the observed structure of the Arctic Ocean and a conceptual model of how brine release from freezing polynyas maintains the Arctic halocline. From Aagaard et al. (1981).

Satellite-based measurements of polynya areas may constitute a major source of error in computing ice and dense water production (Cavalieri, 1994; Winsor and Björk, 2000). The principal sources of error result from inaccuracies in measuring the open water area (polynya size), in estimating the meteorological parameters (near-surface air temperature, humidity, wind speed), and in using bulk formulae parameterizations to calculate the heat and moisture fluxes. Another source of error results from neglecting the heat loss over thin ice areas (Figure 1.2).

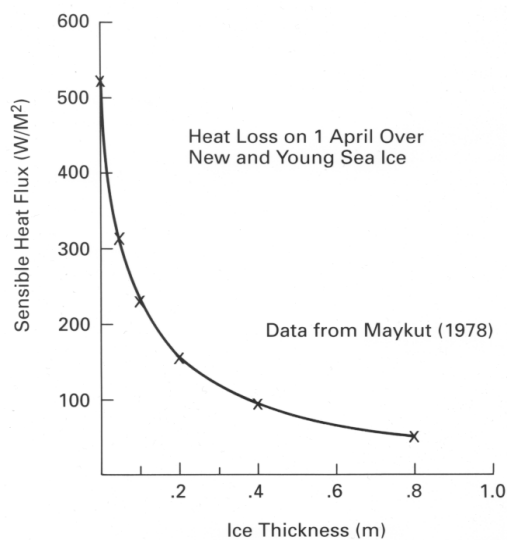


**Figure 1.2** Heat loss on April 1 over new and young sea ice based on data from Maykut (1978).

Furthermore, modeling studies have shown that the correct parameterization of both the polynya forcing areas (open water area) and the polynya forcing fall-off region (thin ice area) is important to the understanding of the production of dense water and its transport across the continental shelf (Gawarkiewicz and Chapman, 1995). Our approach will consist of a series of aircraft flights over selected coastal polynyas to make sea ice concentration, sea ice type, and heat and moisture flux measurements at different altitudes over the polynya and at different distances downwind coordinated with AMSR-E measurements. Specific details of the objectives and methodology are described in the following sections.

## 2 OBJECTIVES

### 2.1 Sea Ice Validation Objectives

The prime objective of the sea ice validation program is to establish statistical relationships between the sea ice parameters derived from the new AMSR-E sea ice algorithms and those same parameters derived from other data sets covering as many geographical areas as possible for different seasons. These parameters include sea ice concentration, and temperature for both hemispheres, and snow-depth on sea ice for the southern polar region and the northern polar seasonal sea ice zones only. Other objectives are to understand the limitations of each algorithm including the reasons for their particular level of performance in different regions and under different conditions, to understand the differences between the NT2 and ABA retrievals, and to suggest improvements to each of the algorithms based on the results of the validation studies.

#### 2.1.1 Validation Criteria

The validation criterion to be used is that the derived AMSR-E sea ice products agree on average with the corresponding validation data set to within the estimated accuracy of the validation data set. The validation data sets will be derived from any one or a combination of field, aircraft, and high-resolution visible and infrared satellite data and are expected to provide a more accurate measure of the standard sea ice products than the AMSR-E retrieved products. The underlying philosophy of this approach is that confidence in the sea ice products derived from the AMSR-E will be achieved by showing consistency of such products with independently derived data that are spatially and temporally coincident (Comiso and Sullivan, 1986; Cavalieri, 1991; Cavalieri, 1992; Steffen and Schweiger, 1991; Grenfell et al., 1994).

#### 2.1.2 Accuracy Goal

Our accuracy goal for each of the sea ice products is based on extensive experience with satellite multichannel passive microwave radiometer data. Table 2.1 summarizes previous validation results from SMMR and SSM/I. These goals are provided below for each standard product.

**Sea ice concentration:** Based on our experience with the SSM/I, the anticipated accuracy of AMSR-E sea ice concentrations will range from 4% to 10%, while that of sea ice concentrations from high resolution satellite and aircraft sensors can be significantly better. The higher the spatial resolution the less significant are errors caused by signature ambiguities within a pixel, particularly when integrated over an AMSR-E footprint. For example, the accuracy of sea ice concentrations derived from cloud free

Landsat MSS imagery is estimated to be in the range of 2-4% (Steffen and Schweiger, 1991). Biases relative to the validation data can be reduced through the adjustment of the algorithm tie-points. Our accuracy goal for sea ice concentration ranges from 4% during the dry winter months to 10% during late spring and summer when surface wetness and meltponding make the emissivity of sea ice highly variable both spatially and temporally. Ultimately, we would like to achieve a 4% accuracy for all regions and seasons.

**Table 2.1** Quantitative Estimates of Algorithm<sup>+</sup> Accuracy Based on Comparisons With Other Sources of Ice-Concentration Measurements (from Gloersen et al., 1992)

Region	Month	Sensor	Mean Diff. $\pm 1$ SD	Ref. Data Set	Ref.
<u>Total Ice Concentration</u>					
Bering Sea	Feb	SMMR	$\pm 5\%$ (Thick FY)	Ship reports	(1)
Baffin Bay	Mar-May	SMMR	-3.5%	Landsat MSS	(2)
Baffin Bay	Jun	SMMR	-10%	Landsat MSS	(2)
Beaufort Sea	Oct	SMMR	$-1.5\% \pm 2.6\%$	Landsat MSS	(3)
Weddell Sea	Oct	SMMR	$0.3\% \pm 7.6\%$	SIR-B	(4)
Beaufort & Chukchi Seas	Sep-Nov	SSM/I	$0.6\% \pm 7.4\%$	Landsat MSS	(5)
Beaufort Sea	Mar	SSM/I	$-2.1\% \pm 3.1\%$	Landsat MSS	(5)
Bering Sea	Mar	SSM/I	$-9.4\% \pm 6.1\%^{++}$	Landsat MSS	(5)
Greenland Sea	Sep	SSM/I	$-3.7\% \pm 1.4\%$	Landsat MSS	(5)
Weddell Sea	Nov	SSM/I	$-1.1\% \pm 3.1\%$	Landsat MSS	(5)
<b>Summary</b>		SSM/I	$-3.6\% \pm 6.6\%$	Landsat MSS	(5)
Amundsen Sea	Dec	SSM/I	$1.3\% \pm 3.6\%$	Landsat MSS	(5)
Beaufort & Chukchi Seas	Mar	SSM/I	$-2.4\% \pm 2.4\%$	NADC/ERIM SAR & NOARL KRMS	(6) (6)
<u>Multiyear Ice concentration</u>					
Beaufort & Chukchi Seas	Mar	SSM/I	$5\% \pm 4\%^*$ $12\% \pm 11\%^{**}$	NADC/ERIM SAR & NOARL KRMS	(6) (6)
Beaufort Sea	Mar	AMMR	$-6.0\% \pm 14\%$	JPL C-band SAR	(6)
(1) Cavalieri et al. (1986)			<sup>+</sup> The algorithm has been used with SMMR, SSM/I, and AMMR data.		
(2) Steffen and Maslanik (1988)					
(3) Steffen, unpubl. data (1990)			<sup>++</sup> Including new ice.		
(4) Martin et al. (1987)			<sup>*</sup> Excluding data from 1 of the 4 flights which gave anomalously large and unexplained biases.		
(5) Steffen and Schweiger (1991)					

(6) Cavalieri et al. (1991)	**Including data from all 4 flights.
-----------------------------	--------------------------------------

**Sea ice temperature:** The expected accuracy of sea ice temperatures derived from AMSR-E is estimated to be about 4K based on our experience with the Nimbus 7 SMMR. This estimate is largely dependent on the accuracy of the retrieved sea ice concentration and on the variability of the sea ice emissivity at 6 GHz. This product represents the physical temperature of the radiating portion of the ice that provides the observed microwave signal. Generally, for first-year ice, the radiating portion is the snow-ice interface, whereas, for multiyear ice, the radiating portion is a weighted mean of the freeboard layer of the ice. The validation data set will be derived using a combination of satellite infrared data, surface field measurements including buoy data, and an ice thermodynamics model. Our accuracy goal for sea ice temperature is 4 K or better.

**Snow depth on sea ice:** The algorithm uses regression coefficients to derive snow depth on sea ice in seasonal sea ice regions to an estimated regional accuracy of about 4 cm based on our experience with the SSM/I (Markus and Cavalieri, 1998). A comparison of snow depth distributions from ship measurements and from SSM/I snow depth retrievals in the Southern Ocean suggests that the SSM/I retrievals underestimate the in situ measurements by 3.5 cm and that the rms difference is about 4 cm. The underestimate results from microwave signal saturation at snow depths of about 50 cm so that snow depths greater than this cannot be detected with the current algorithm. On average, snow depths over first-year ice in the Arctic are typically less than this, but if necessary this limitation may be circumvented by the additional use of the 6 and 10 GHz channels. Temporal information is used to filter retrievals that have been affected by freeze-thaw processes using a threshold of 5 cm per day. Thus, our accuracy goal for snow depth on sea ice is 5 cm. Under winter conditions, the accuracy may be better.

## 2.2 Arctic Coastal Polynya Objectives

### 2.2.1 Satellite Measurement of Coastal Polynyas

There are two important objectives that will be addressed. The first objective is to assess the accuracy to which the AMSR-E sea ice concentration algorithms can map the size of coastal polynyas and to measure the degree of low ice concentration bias, if any, resulting from the presence of thin ice. Previous studies of Arctic coastal polynyas using SMMR and SSM/I sea ice algorithms (e.g., Cavalieri and Martin, 1994) may have overestimated polynya areas by up to 40% (Winsor and Björk, 2000). On the other hand, these observational studies measure only the open water area of the polynya and neglect the polynya thin ice areas. Neglecting areas of thin ice results in an underestimate of the sensible heat loss from ocean to atmosphere during winter. Figure 1.2 illustrates the magnitude of heat loss over new and young sea ice in winter. The higher spatial resolution of AMSR-E relative to SMMR and SSM/I is expected to greatly improve the mapping of coastal polynyas.

### 2.2.2 Surface Heat and Moisture Flux Measurements

The second objective is to measure directly surface heat and moisture fluxes over coastal polynyas to evaluate the parameterizations currently used in bulk formulation models and to measure the fall off of these fluxes downwind. A related issue is how the fall off of these fluxes downwind of the polynyas are related to the increase in sea ice concentration and ice thickness. The spatial dimensions

of both the ‘forcing’ (open water area) and the ‘forcing decay’ (thin ice area) regions of the polynya are important parameters in theoretical models of dense water formation and its transport across the Arctic shelf (e.g., Gawarkiewicz and Chapman, 1995).

### **3 VALIDATION DATA SOURCES**

The relatively large footprints of the AMSR-E sensor, the variable nature of sea ice over space and time, and the complex logistics associated with polar operations make the sea ice products particularly difficult to validate. The validation program for sea ice will therefore rely heavily on the analysis of coincident sea ice data sets from aircraft and satellite. Coordinated surface and aircraft measurements will be particularly important for providing the validation data for snow depth and sea ice temperature. The spatial resolutions of the comparison data sets range from the 25-m Landsat 7 ETM+ imagery at the high resolution end, to 100-m (at nadir) aircraft passive microwave imagery, and 1-km resolution AVHRR imagery. High (meter- to sub-meter) resolution aerial digital photographs and video from the P-3 and from uninhabited aerial vehicle flights will augment these data. The spatial resolutions of the level 3 sea ice products are 12.5 km and 25 km.

#### **3.1 Satellite**

##### **3.1.1 Passive and Active Microwave**

In addition to EOS Aqua AMSR-E, several other satellite multichannel microwave imaging radiometers will be in orbit within the next year. This will allow an intercomparison of sea ice retrievals from the different radiometers and will provide a basis for assessing retrieval differences resulting from differences in calibration and in diurnal variations. Current and anticipated satellite passive microwave sensors in addition to AMSR-E include:

- (a) ADEOS II AMSR launched on December 14, 2002.
- (b) Special Sensor Microwave/Imager (SSM/I) on the DMSP F13, F14, and F15 spacecraft.
- (c) Special Sensor Microwave Imager/Sounder (SSMIS) to be launched in 2003 on the DMSP F16 spacecraft.

Active microwave satellite sensors are more limited in their usefulness, because of the inherent difficulties of resolving backscatter ambiguities, but are potentially valuable sources of data for validating sea ice extent and ice type (first-year and multiyear). These sensors include high-resolution RADARSAT and QuikSCAT and will be particularly useful in areas of persistent cloud cover and during periods of polar darkness where visible and IR sensors can not be used.

##### **3.1.2 Visible/IR**

Under favorable conditions, high-resolution visible and infrared sensors including for example Landsat-7 ETM+, DMSP OLS, ADEOS II GLI, NOAA AVHRR, and MODIS (both Terra and Aqua) imagery will be acquired. Landsat 7 ETM+ imagery is particularly useful with its 25-meter spatial resolution (including a 15-meter panchromatic band). This high resolution capability has been used to identify melt features such as melt ponds, which cause low ice concentration biases in the AMSR-E algorithms (Markus et al., 2001). Landsat imagery has also been used for the validation of Nimbus 7

SMMR and DMSP SSM/I sea ice data sets (Steffen and Schweiger, 1991; Steffen and Maslanik, 1988) as well as in sea ice algorithm comparisons (Steffen et al., 1992; Comiso et al., 1997).

## 3.2 Aircraft

### 3.2.1 NASA WFF P-3B

A key component of the validation effort is the acquisition of high resolution passive microwave radiometer data at the same frequencies and polarizations as those measured by AMSR-E. The platform for acquiring these data will be the NASA Wallops Flight Facility (WFF) P-3B aircraft (Figure 3.1). The P-3 aircraft is a 4-engine turboprop capable of long duration flights of 8-12 hours, large payloads up to 15,000 pounds, altitudes up to 30,000 feet and true airspeeds up to 330 knots. More detailed information may be obtained from the Web site [www.wff.nasa.gov](http://www.wff.nasa.gov). A summary of the performance of this aircraft is reproduced from the Web site and is given in Table 3.1.



**Figure 3.1** NASA WFF P-3B aircraft.

**Table 3.1.** NASA WFF P-3B Altitude, range and airspeed matrix.

	High Altitude 5-30K Feet	Medium Altitude 10-25K Feet	Low Altitude 500-10K Feet
Endurance (Hours)	12	10	8
Range (Nautical Miles)	3,800	3,000	2,400
Speed (Knots)	330	300	270

#### 3.2.1.1 Passive Microwave Radiometry

The passive microwave radiometer to be used for the field campaign is the NOAA Environmental Technology Laboratory (ETL) Polarimetric Scanning Radiometer (PSR). The PSR

system simulates all the AMSR-E bands and is compatible with the Wallops P-3 aircraft. A summary of the PSR specifications is given in Table 3.2.

**Table 3.2** Polarimetric Scanning Radiometer specifications.

SCANHEAD	FREQUENCIES (GHz)	POLARIZATION	BEAMWIDTHS
PSR/A	10.6-10.8	v,h,U,V	8°
	18.6-18.8	v,h,U,V	8°
	21.4-21.7	v,h	8°
	36-38	v,h,U,V	2.3°
	86-92	v,h,U	2.3°
PSR/CX	5.82-6.15	v,h	10°
	6.32-6.65	v,h	10°
	6.75-7.10	v,h,U,V	10°
	7.15-7.50	v,h	10°
	10.6-10.8	v,h	7°
	10.68-10.70	v,h	7°

### 3.2.1.2 Snow Radar

The snow radar (currently under development by S.P. Gogineni, T. Markus, and G. Prescott) will be an airborne stepped frequency pulse radar operating in the frequency range of 2 to 18 GHz. The anticipated vertical resolution is 2 cm. The proposed instrument provides the only means to measure adequately snow depth at spatial scales comparable to the AMSR-E. First tests of this instrument over sea ice will take place in October 2003 on the Australian research icebreaker Aurora Australis in East Antarctica. Radar development (hardware and software) is anticipated to be completed in time for the 2005 Arctic field campaign.

### 3.2.1.3 Infrared Radiometry and Photography

NASA Langley Research Center will operate a nadir viewing PRT-5 infrared radiometer. Aerial photography will be provided by NASA Wallops video and digital cameras for the characterization of surface conditions. In addition, a video camera and an IR radiometer (9.6-11.5  $\mu\text{m}$ ) will be boresited with the PSR radiometers.

### 3.2.1.4 Gust Probe System

The NASA Langley Research Center Turbulent Air Motion Measurement System (TAMMS) on the WFF P-3 is composed of several subsystems including: (1) distributed pressure ports coupled with absolute and differential pressure transducers and temperature sensors, (2) aircraft inertial and satellite navigation systems, (3) a central data acquisition/processing system, and (4) water vapor instruments and potentially other trace gas or aerosol sensors.

The angle of ambient airflow relative to the aircraft is determined using the five-hole pressure port technique as described by Brown et al (1983). For this technique, five flush pressure ports (each with a diameter of  $\sim 0.6$  cm) have been integrated into the P-3 radome in a cruciform pattern. Flow angle measurements, angle of attack and sideslip, are obtained from differential pressure measurements made between the pair of vertically aligned ports and horizontally aligned ports, respectively. The center hole is linked to existing static pressure ports on the side of the fuselage to provide required dynamic and total pressure measurements.

The differential pressure fluctuations can then be used to calculate the  $u$ ,  $v$  and  $w$  velocity components relative to the aircraft. Combining these measurements with information from the Inertial Navigation System (INS) allows the calculation of the wind velocity components with respect to an earth-based coordinate system. A Global Positioning System (GPS) is used to correct for long-term drifts in the INS.

Air temperature measurements needed to determine true air speed,  $U_a$ , as well as heat flux are made within a non-deiced total air temperature  $T_t$  sensor housing using a fast-response platinum sensing element (E102E4AL).

A Lyman-Alpha hygrometer manufactured by Atmospheric Instrumentation Research, Inc (model AIR-LA-1AC) is used to provide fast response water vapor measurements. A slower response General Eastern 1011B hygrometer designed for airborne applications is mounted in close proximity and used to normalize the Lyman-Alpha signal. The Lyman-Alpha instrument will be upgraded with a new fast response water vapor sensor for the field program proposed for 2003.

The fluctuations in velocity ( $u'$ ,  $v'$ ,  $w'$ ), the air temperature ( $T'$ ) and water vapor ( $q'$ ) are recorded at a frequency of 20 Hz by an onboard data system. These values are then used to calculate turbulent fluxes of momentum ( $u'w'$ ,  $v'w'$ ), heat ( $T'w'$ ), and moisture ( $q'w'$ ) using the covariance method.

In addition to the output of TAMMS system sensors, display of three-dimensional winds will also be provided in near real time aboard the aircraft. Work is underway to incorporate the aircraft true airspeed and vertical velocity correction algorithms into the TAMMS data acquisition software so that winds of relatively high accuracy can be calculated from the raw input signals. There are plans to provide wind information at 0.1 second intervals to facilitate direct calculation of meteorological fluxes.

### 3.2.2 NSF Aerosonde UAV

As noted earlier, a need exists to map the surface at very high resolution and below cloud cover as well as to obtain atmosphere column information coincident with AMSR-E and P-3 overpasses. Aerosonde Uninhabited Aerial Vehicles (UAVs) can provide these capabilities. The Aerosonde is a small, robotic aircraft designed to undertake a wide range of operations in a highly flexible and inexpensive mode (Holland et al. 1992; Holland et al., 2001). The aircraft, developed by an US-Australian consortium, entered limited operations in 1999. Current operations and further development are being undertaken by *Aerosonde Robotic Aircraft* and *Aerosonde North America* (See [www.aerosonde.com](http://www.aerosonde.com) for details.) The Aerosonde conducts a defined mission in a completely robotic mode. However, all flights are under the command of a ground controller who can change missions and

respond to air traffic control requests. An NSF-funded project as part of the Office of Polar Programs' Long Term Observations program is now underway at Barrow to deploy Aerosondes for routine mapping and atmospheric sounding missions (J. Curry, PI; J. Maslanik, Co-PI). The validation effort will take advantage of these operations See <http://paos.colorado.edu/~curryja/aerosonde/index-frame.html> for more information. Specifications and performance of the Aerosonde are as follows:

**Table 3.3** Specifications and Performance for the Operational Mark 2 Aerosonde

<b>Aerosonde Specifications</b>	
Weight	14 kg
Wing Span	2.9 m
Engine	24cc fuel-injected pusher-prop.
Navigation	GPS, DGPS
<b>Aerosonde Performance</b>	
Speed	Cruise 18-32 m s <sup>-1</sup> ; climb 2.5 m s <sup>-1</sup>
Range	>3000 km (with 1 kg payload)
Endurance	>30 h
Altitude Range	20->7000 m (intermediate weight payload)
Communications	UHF radio, low earth orbit satellite
Payload	2 kg with full fuel load; 5 kg maximum
Instrumentation	Air temperature, pressure, humidity (Vaissala sensors), digital photography (Olympus C-3030 camera), infrared temperature (Heitronics KT-11 pyrometer), aircraft icing sensor, video camera with short-range transmission. A laser altimeter is expected to be available by spring 2003

Aerosondes operate in fully robotic mode, using onboard avionics and pre-programmed flight plans. Radio communication can be maintained with the aircraft via UHF ground link and/or via low earth orbit satellite. The latter allow flights well beyond UHF radio range of approximately 200 km. Testing is underway using LEO satellites (Iridium system) for Barrow-based operations. Up to three Aerosondes can be operated simultaneously to increase the effective payload per mission and to acquire coincident data at different altitudes.

For the AMSR-E validation effort, the types of data to be available from UAV flights will include:

- ? profiles of air temperature, pressure, and humidity.
- ? detailed photographic imaging of surface features at sub-meter resolution;
- ? skin temperatures along flight tracks;
- ? estimation of sea ice concentration, ice type, surface roughness, lead fraction, ridging fraction, and approximate ice thickness using a laser altimeter;

Flights will be conducted from the NARL airfield near Barrow. Typical flight patterns include atmospheric soundings at various locations along the flight tracks, and surface mapping missions at various altitudes. The majority of the flight hours will be dedicated to extended transects flying at relatively low altitude (200 to 400 m) for mapping of surface conditions. A typical pattern to provide

statistics regarding surface conditions would involve 5 east-west flight tracks of 150 km length each, spaced evenly at 25-km apart. Such missions would require approximately 10 hours of flight time. When cloud cover is present, and for selected clear-sky cases, the flight plan will include stacked patterns (for example, below and above cloud cover) to acquire data needed to assess the effects of the atmospheric column and clouds on AMSR-E product accuracy.

A second mode will involve maintaining coverage over specific, localized areas for long durations, spanning approximately 20 hours. This continuous data collection over regions of dynamic or newly-forming ice will allow us to study how changes in pack ice and atmospheric conditions affect a time series of AMSR-E data from multiple Aqua overpasses. As discussed earlier, the two sea ice algorithms have different sensitivities to atmospheric and surface conditions, so data are needed to assess how these differences affect the products. The mission plans will focus on observing the pack ice under a range of weather and ice conditions coincident with Aqua overpasses. Details of flight operations are given in Section 4.

### 3.3 Surface

#### 3.3.1 Barrow

The in situ data collection effort will begin with a general mapping of Barrow-area fast ice conditions prior to the P-3 flights and surface measurements using satellite SAR imagery if available, augmented by information from local ice experts and aircraft reconnaissance (Figure 3.2). This ice mapping will then be used to identify specific ice conditions for subsequent surface measurement. Although the precise coverage will vary depending on local conditions, the likely areas to be sampled will lie within 25 km of Barrow for *in situ* measurements on fast ice, with a typical maximum extent of fast ice of about 20 km from shore.

The shore-fast ice along the north coast of Alaska, particularly near Barrow, generally includes most of the major sea ice and snow classes found further north in the Arctic Basin, albeit in smaller units or floes. The fast ice parallels the coast and tends to have a banded structure, but by ranging parallel to the coast, we intend to sample a sufficient number of floes of suitable size for representative ice and snow conditions. These sampling locations will be augmented by making measurements on the saline ice which covers Elson Lagoon (an area of approximately 15 km by 50 km consisting of uniform first-year ice) and fresh-water ice on lakes in the Barrow area. The relatively fine resolution of the NASA P-3 PSR imagery will result in pure-pixel observations over the sample locations. Results of the comparisons between field conditions and brightness temperatures observed by the P-3 can then be scaled up to be appropriate to AMSR-E resolutions.

Our sampling strategy will be to make a preliminary identification of suitable floes in each ice and snow class in the fast ice zone as noted above. We will then visit these target floes during a reconnaissance traverse. Based on observed surface characteristics and sampling, we will identify the set of floes to be targeted by the aircraft (P-3 and Aerosondes). A stratified sampling technique will be used to help assure adequate sampling over the various surface types available. The measurement strategy will take advantage of experience gained during the Surface Heat Budget of the Arctic (SHEBA) experiment, where the investigators developed an efficient system for traversing and making measurements on ice. During SHEBA, over 500 km in 20 km legs were surveyed using snow machines. No suitable aircraft are presently in place for lease in the Barrow area to assist in the sampling. A small

helicopter (a Bell-47) may be available for some reconnaissance and sampling work, although the flight area is limited to fast ice only, and only one passenger and minimal gear can be carried.

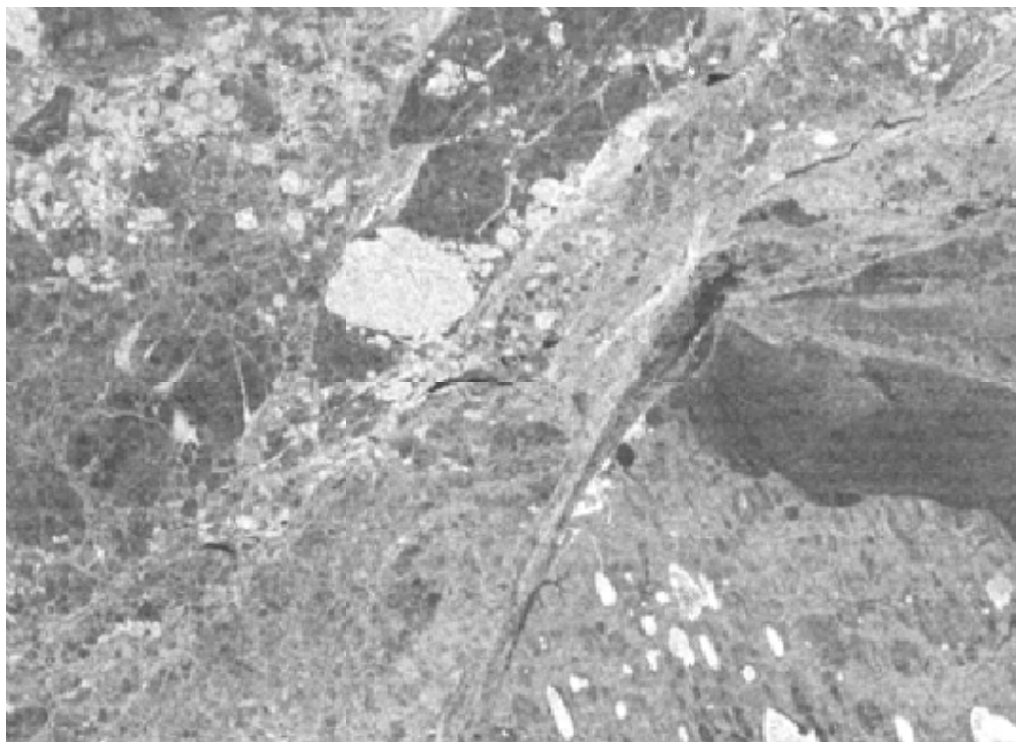


**Figure 3.2** The Barrow in situ study area, illustrating variations in sea ice and land conditions apparent in synthetic aperture radar data (RADARSAT image courtesy RadarSAT International).

A key element of the Barrow-area effort is the use of data collected at multiple scales as a means to extrapolate limited in situ data to larger areas. It is thus imperative that it be possible to match observation locations among the in situ, aircraft, and satellite data. GPS and collection of ground control points (GPS locations of particular features) will assist with this. However, we will also investigate the potential of devices such as point-source microwave transmitters, flares, targets, or other means that could be deployed on the ice to help improve the co-registration of different data sets.

A variety of tools developed over the past few years will be used to quickly, efficiently, and adequately sample those target floes for which we plan to obtain aircraft data. A GPS base station will be set-up and operated at NARL near Barrow. All snow and ice measurements can thus be associated with precise GPS positions. Measurements will be made along multiple traverse lines spanning the floes (or ridges in the case of deformed ice), and in some cases, on a grid network on individual floes. Near-continuous measurements of snow depth will be made using an automatic snow depth probe which we have developed (U.S. Patent 4600842) and a sled-mounted FM-CW X-band radar (Holmgren et al., 1998). An up-grade to the radar has just been completed which allows the radar system to collect snow depth and GPS position data simultaneously, permitting mapping of considerable areas of the snow cover on the ice in detail. In addition to providing direct comparison data for PSR and the AMSR-E

algorithms, the transects of radar-derived snow information will be useful for interpreting the planned aircraft snow radar if funding is available for an in situ campaign during 2005.

Closely-spaced (every 0.5 m) measurements of the snow-ice interface temperature will be made on traverse lines using thin probes (Patent 5815064). Continuous measurements of snow temperatures will be recorded using mini-data loggers (Onset Computer Corp.) installed at the start of the intensive field campaign. At frequent intervals along traverse lines, snow texture, snow grain size, snow stratigraphy, and snow/ice interface temperatures will be determined in snow pits. At SHEBA (Sturm and others, in press) and in the Antarctic (Sturm and others, 1998) developed methods that allow rapid identification and quantification of snow characteristics. These methods will be used and improved upon for the planned work. At snow pit locations, ice thickness will be determined by drilling through the ice, and ice cores will be obtained from a sub-set of these locations for later analysis of ice type, brine pocket density, and percentage snow-ice, if any, and other properties needed for interpretation and modeling of microwave emission. Snow/ice profile temperatures will be obtained at selected locations using thermistor chain systems employed by D. Perovich.

In addition to these surface measurements, the validation effort in the Barrow area will take advantage of the ground-based remote sensing data obtained by the Dept. of Energy's Atmospheric Radiation Monitoring (ARM) site (<http://www.arm.gov/docs/sites/nsa/nsaaao.html>) and NOAA's Climate Monitoring and Diagnostics Laboratory site near Barrow (<http://www.cmdl.noaa.gov/obop/brw/index.html>), and the National Weather Service station in Barrow. These ongoing operations provide atmospheric state variables, vertical profiles, radiative fluxes, and cloud information. These data, along with atmospheric information acquired by Aerosondes and the P-3, will be used to assess the performance of atmospheric corrections and as input to modeling. We also intend to make use of the available suite of ice and atmospheric information collected during the SHEBA experiment. These data will, in particular, be useful for refining radiative transfer and ice temperature modeling.

### **3.3.2 Navy Ice Camp**

Additional measurements will be made at an ice camp that will be installed by the U.S. Navy. This camp will be located in the Beaufort Sea. The camp is scheduled to be deployed on or about March 17th, leaving a window of 5 days during which the NASA P-3 will be in Alaska and the camp location will have been determined and fixed. As soon as the camp can be occupied, science personnel will proceed to the camp. At the camp, it is anticipated that extensive measurements of snow depth and ice thickness will be made on one or several lines of 1 to 3 km length. It is likely that both first-year and multiyear ice will be present near the camp, so both of these ice types will be sampled. At the current time, it is anticipated that snow depth will be measured using hand and automatic probes, and that ice thickness will be measured using the EM-31 and checked by drilling holes. Only limited snow properties (layers, density) will be recorded, and there are no plans to take ice cores. A coordination meeting hosted by the Navy is planned for February 10, 2003. At that meeting, we plan to discuss protocols for how the camp location will be transmitted to the NASA team, how line orientation will be decided, and whether laser altimetry from the aircraft is desired.

### 3.3.3 Nome

We are investigating the feasibility of carrying out Aerosonde operations based at Nome, to complement the P-3 flights over the Bering Sea during 2005. No concurrent in situ measurements are planned at this point.

### 3.3.4 Other Field Programs of Opportunity

Plans by other groups for experiments that could contribute to the AMSR-E validation effort are continuing to evolve. These include proposals for detailed study of the Barrow-area fast ice, a possible ice-research camp in the Beaufort Sea in 2003, and the Ross Island Meteorology Experiment (RIME) under consideration for 2003-2005. We intend to follow the progress of these plans, and will attempt to capitalize on such efforts where possible.

## 4 APPROACH

### 4.1 Sea Ice Validation Approach

The approach for meeting the validation objectives is one of compiling and analyzing spatially and temporally coincident data sets for comparison with the AMSR-E sea ice parameters. Another key element in the approach is the utilization of modeling and sensitivity studies (section 5). Coincident or nearly coincident observations will be obtained from surface measurements, coordinated NASA and NSF Aerosonde UAV underflights covering several AMSR-E footprints, and from other satellite sensors. While the focus of the planned aircraft campaigns is on winter conditions, we intend to take advantage of pond statistics derived from Aerosonde flights planned as part of the ongoing NSF effort in Barrow to assist in the validation of AMSR-E sea ice concentrations during the melt season. During June/July 2000, an AMSR-E prelaunch aircraft campaign called Meltpond2000 (Cavalieri, 2000) was undertaken to validate the NT2 algorithm under melt conditions using the airborne PSR system, but because of problems with the 89 GHz V-pol. channel validation with aircraft data could not be undertaken. Instead, Landsat 7 ETM+ imagery is currently being used.

The Arctic regions selected for the aircraft campaigns were chosen because they give rise to the largest retrieval errors during the winter season. A more detailed discussion of the attributes of each region is provided in sections 4.1.1 and 4.1.2 below. The approach is necessarily sea ice product specific. The following is a summary of the validation methods to be used for each standard product.

**Sea Ice Concentration:** The primary approach for the validation of retrieved AMSR-E sea ice concentrations is to utilize data from dedicated aircraft campaigns in conjunction with high resolution satellite data, including those from Landsat 7, Terra and Aqua MODIS and ASTER, NOAA AVHRR, DMSP-OLS, RADARSAT, and scatterometers. The P-3 aircraft data will provide high-resolution measurements of brightness temperatures and subsequently ice concentrations for selected regions, whereas the visible and IR satellite data provide for wider spatial and temporal coverage (Figure 4.1). An example of the type of comparison that will be undertaken with Landsat 7 ETM+ data is illustrated in Figure 4.2.

Digital imagery from the Aerosonde flights will depict surface conditions at sub-meter resolution. Surface skin temperature profiles acquired by the Aerosonde yield comparison data for ice temperatures and provide information on thin-ice coverage and presence of leads. Variations in spectral albedo (for the visible channels) or changes in surface temperature (for the infrared data) can be used for proxies not only of ice concentration but also of ice thickness. The focus of the P-3 campaigns will be on those regions that exhibit large retrieval errors based on past studies. Although aircraft passive microwave data provide essentially the same type of information as the AMSR-E, the much higher spatial resolution will allow the identification of pure surface types and direct comparison with in situ measurements, and therefore the investigation on how specific surface types translate in the sea ice concentration retrievals. Furthermore, with varying aircraft altitude, the dependence of the atmospheric contribution on the retrievals can be studied. High-resolution active microwave satellite systems, such as RADARSAT, are most useful during persistent cloud cover and during polar darkness. Data from microwave scatterometers, such as those from QuikSCAT, will be utilized for identifying areas of divergence and ice drift. However, data from active systems are more difficult to interpret than those from passive and visible systems, because of unpredictable backscatter from different ice types, from open water within the ice pack, and from wind-roughened seas.

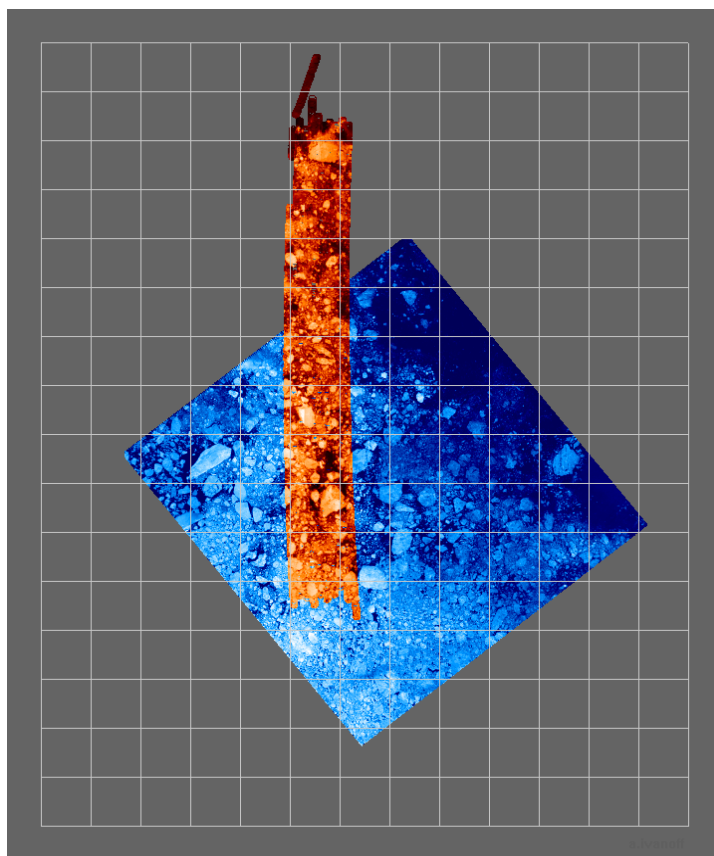


**Figure 4.1** Landsat 7 ETM+ Image of Baffin Bay with NOAA ETL Polarimetric Scanning Radiometer brightness temperature (19 GHz, V pol.) mosaic overlain (outlined in black) for June 27, 2000. The Landsat and microwave data are gridded at a resolution of 0.5 km. The 25-km SSM/I grid is also shown for comparison.

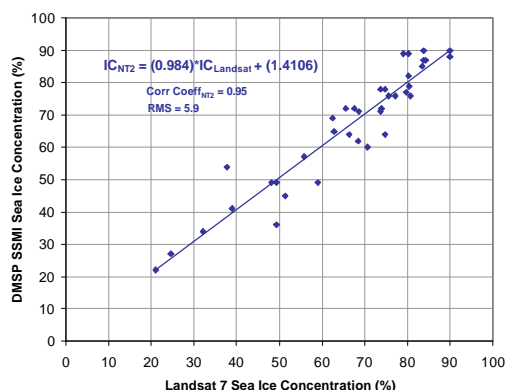


**Figure 4.2** Comparison of DMSP SSM/I and Landsat 7 ETM+ sea ice concentrations for June 27, 2000 during Meltpond2000. The ETM+ image is shown in Figure 4.1.

One important aspect of the sea ice concentration validation is the effect of weather on the sea ice concentration retrievals. This is particularly important for those retrievals derived from the NT2 algorithm which makes use of the AMSR-E 89 GHz channels. To this end, we are planning a series of Aerosonde UAV flights for the purpose of mapping surface characteristics under a variety of atmospheric conditions. These will be coordinated with the NASA P-3 flights and will occur both above and below the cloud cover. The coordinated data collection effort (including the P-3, Aerosondes, surface sampling, and surface-based remote sensing) is designed to provide a suite of data extending from the surface through the atmosphere to an altitude of about 6 km. In addition to general mapping of surface features, the data collection plan is intended to support analysis of the effects of the atmospheric column and of short-period temporal variations in surface conditions on AMSR-E brightness temperatures. The UAV flights will provide profiling of the atmospheric column and transects measuring sea ice conditions out from the Alaskan coast to a distance of about 1500 km. Atmospheric observations from NOAA and DOE facilities near Barrow will provide additional data for establishing atmospheric conditions during these underflights.

Another concern is the sensitivity of the ice concentration retrievals to sea ice temperature variability. This issue will be addressed both from algorithm sensitivity analyses and from closely-spaced in situ snow-ice interface measurements made along Barrow-based transects and from temperature profiles in the ice/snow column provided by thermistor chains. These transects will be overflown by the P-3 aircraft. The P-3 will provide high-resolution measurements of brightness temperatures and surface temperatures using an IR radiometer. Details of the aircraft instrumentation are presented in section 3.2 and those of the surface measurements are presented in section 3.3.

**Sea Ice Temperature:** Sea ice temperature will be obtained using the ABA algorithm. For first-year sea ice, the ice temperature derived from the vertically polarized 6.9 GHz channel represents the temperature of the sea ice surface at the snow/ice interface, because at this frequency the snow cover is transparent to the radiation. For multiyear ice, the derived sea ice temperature represents a weighted-average of the freeboard portion of the ice. The primary technique for the validation of AMSR-E ice temperature is to make use of empirical relationships between the ice temperature and snow surface

temperature in comparison with aircraft and satellite (i.e., MODIS and AVHRR) thermal infrared data. Sea ice temperature retrievals obtained with the high-resolution P-3 aircraft microwave radiometers will also be compared with the Barrow-based surface transect measurements and thermistor-chain vertical profiles to assess errors associated with the use of empirical parameters. Further refinements of the empirical parameters will be made as more field data become available and through the use of a thermodynamic model of sea ice and snow.

The retrieved ice temperatures will be further validated using surface temperature data from Arctic buoys and other platforms. While these are only point measurements, arrays of buoys exist and they provide continuous measurements that can be used to check the temporal consistency of the derived AMSR-E temperature data. The temperature algorithm was developed through the use of 6.6 GHz data that were observed by the Nimbus-7 SMMR and historical buoy and field data. The SMMR data, however, have limited value for testing the effectiveness of the AMSR-E algorithm because of very large footprint and instrumental problems associated with polarization mixing.

**Snow Depth on Sea Ice:** Because in situ snow depth observations over sea ice are so sparse and because surface measurements are so costly to acquire, the validation strategy is to utilize an airborne sensor to measure snow depth on sea ice. While the planned in situ snow depth measurements on Barrow fast ice will provide data to validate the algorithm using the P-3 PSR radiances, the airborne radar is the only way to provide the spatially and temporally coincident measurements needed to validate snow depth over large areas commensurate with the 12.5-km snow depth product resolution. As noted previously, an airborne radar with the capability to measure snow depth is currently under development. The development and testing of this radar is expected to occur in time for the 2005 aircraft campaign. For the 2003 campaign, our approach will be to obtain the snow depth retrievals using the P-3 airborne microwave radiometers and to compare these retrievals to the Barrow-based in situ snow depth measurements. In addition to snow depth, snow texture, grain size, and snow stratigraphy will be measured to help understand the sensitivity of the algorithm to these parameters and to make algorithm improvements. Available snow depth measurements made from ships such as those compiled by Markus and Cavalieri (1998) will be used to help validate the AMSR-E snow depth retrievals. Qualitative checks will also be made through comparisons with AMSR-E ice type maps and with MODIS, LANDSAT, and AVHRR images.

#### **4.1.1 Beaufort and Northern Bering Seas (March 2003)**

The rationale in selecting these regions for AMSR-E sea ice validation is that the largest errors in winter Arctic sea ice concentration retrievals occur in the seasonal sea ice zones (SSIZs). These very dynamic regions consist of various unresolved ice types and very different sea ice surface conditions. A comparison of the original NASA Team and Bootstrap algorithm retrievals using SSM/I data shows that the Bering Sea is a region showing some of the largest differences in the Arctic (Comiso et al., 1997). These differences result from the wide variety of ice types (new, young, and thin FY ice) and surface conditions (e.g., variations in snow depth) that exist in this SSIZ. In contrast, the microwave signatures of older first-year ice and perennial (multiyear) ice types found in the Beaufort Sea contrast sharply with the Bering Sea ice types. Other validation issues to be addressed in these regions include algorithm sensitivity to sea ice temperature, atmospheric, and snow cover variabilities.

The field campaign consisting of 7 coordinated aircraft flights is expected to take two to three weeks starting early March 2003. Some adjustments may be necessary just prior or during the campaign (e.g., different flight days and different location sites), resulting from unpredictable sea ice and weather conditions. Our tentative flight program is to fly 7 8-hour data flights with the NASA P-3 from Fairbanks, AK over the Beaufort and northern Bering Seas. From Fairbanks flight time to the northern Bering Sea (63°N, 170°W) or to the central Beaufort Sea (75°N, 150°W) will take about 2 hours flying 330 knots at an altitude of 25-30K feet. This leaves approximately 4 hours on site, although the transite legs will also be used for data collection coordinated with surface and Aerosonde measurements near Pt. Barrow. Flight time to Pt. Barrow is only 1 hr 30 min. Specific flight plans are discussed in section 4.3.

In all cases, the specific areas overflown will depend on surface and weather conditions and coordination with the Aerosonde team in Barrow. Near real-time AMSR-E or DMSP SSM/I imagery and possibly RADARSAT quick-look images will be used to guide the flight planning sessions before each flight.

When coordinating with surface and Aerosonde flights, selected flight legs will be done over the same ground track (within the limits of GPS navigation accuracy) at high altitude (ferry altitude) and at low altitude. The low-altitude leg ideally would be beneath any intervening cloud layers, but at a height sufficient to provide an PSR swath width of at least 2 km. This set of tracks is to be done over fast ice near Barrow, coincident with in situ measurements in the same area.

Flights will be timed to be as coincident as possible with EOS Aqua overpasses and with other satellite observations such as with Landsat 7 ETM+. A flight schedule that provides near-coincident coverage from multiple satellites (in particular DMSP SSM/I, RADARSAT, and possibly NOAA AVHRR) is desirable to allow intercomparison of multiple data types. We intend to fly one or more Aerosonde UAVs in concert with most of the P-3 flights.

With regard to the surface heat flux study, both regions contain persistent coastal polynyas that experience very large surface heat losses. We plan to dedicate two of the seven flights over coastal polynyas. The specific flight strategies are discussed in section 4.2.

#### **4.1.2 Bering and Chukchi Seas (Feb/Mar 2005)**

As noted earlier, an airborne radar will be flown on the NASA P-3 along with passive microwave radiometers to provide the required spatial and temporal coverage for the validation of snow depth on sea ice. From previous surface radar measurements (Jezek et al., 1998), snow depth on sea ice has been measured to within an accuracy of about 2 cm, an accuracy more than sufficient for the radar to serve as a validation tool for AMSR-E snow depth retrievals.

The Bering and Chukchi Seas provide a full range of snow depths and snow conditions. Persistent polynyas in the northern Bering Sea and off the Alaskan coast region of the Chukchi Sea provide gradients of snow depth ranging from 0 cm on new ice to 15-20 cm on first-year ice downwind of the polynya. Ridged sea ice areas generally contain much deeper snow. By late February to early March the Chukchi Sea will have an older snow cover with larger grains resulting in greater scattering. This will provide a good area to test the effects of grain size variability on the snow depth retrievals.

We plan to fly 5 flights from Fairbanks, AK over the Bering and Chukchi Seas. If possible, flights will be coordinated with Aerosonde flights out of Nome. High and low altitude patterns will be flown to provide a comparison of snow depth retrievals from AMSR-E and airborne passive microwave radiometers with the snow radar. The plan is to fly mosaic patterns over selected areas while covering as many AMSR-E footprints as possible. These flights will also provide an opportunity to collect additional sea ice validation data not collected during the 2003 field campaign.

## **4.2 Polynya Surface Flux Measurement Approach**

The approach to be used consists of using a gust probe system on the NASA P3 aircraft with the goal of:

- mapping surface heat and moisture fluxes over the St. Lawrence Island polynya in the northern Bering Sea and/or coastal polynyas off the Alaskan coast of the Beaufort Sea,
- measuring how these fluxes change with distance downwind from the polynya and also how they vary with sea ice concentration and ice type,
- using these in situ aircraft data sets to aid in the development of methodologies for estimating fluxes from polynyas using satellite remote sensing data,
- determining the accuracy of flux estimates obtained from Aerosonde flights and bulk formulae.

Flights will be made when synoptic conditions are favorable for large, sustained polynya events. For the St. Lawrence Island polynya, our preferred site, the conditions consist of a large area of high pressure located over Siberia and a low pressure system over the Aleutians. These systems provide northerly surface winds over the Bering Sea forcing the opening of a polynya along the southern coast of the island. A crosswind multi-level stack pattern will be flown over the polynya in order to map the vertical structure of the fluxes over the polynya. Several other crosswind stack patterns will be flown downwind of the polynya to determine the relationship between changes in surface fluxes and sea ice concentration and ice types. 1-second samples of pressure, temperature, dew-point temperature and wind will be made at the following altitudes: 150, 300, and 600 ft, if approval is received as anticipated for transects below 500 ft. A PRT-5 type of downward-looking radiometer will provide surface temperature.

## **4.3 Arctic Flight Operations**

The performance characteristics of the NASA WFF P-3B aircraft is summarized in Table 3.1, while the aircraft instrumentation is discussed in section 3.2.1. The P-3 instrumentation for the Arctic2003 campaign is summarized in Table 4.1. The P-3 will make a total of 7 validation and science flights from Fairbanks International Airport (FAI), Alaska. The regions that will be overflown include the Bering, Beaufort, and Chukchi seas as well as special study sites near Barrow Alaska.

The objectives for each of the 7 flights are summarized in Table 4.2. These objectives include both those for sea ice validation and polynya surface heat and moisture flux studies. The flight lines described here are only approximate. The final lines will depend on the regional weather and ice conditions during March 2003. The tentative lines for the Barrow flights are shown in Figure 4.1 and the flight lines for the other flights (Table 1) in Figure 4.2. Each of the 7 flights will be 8-hours in

duration. The transit time from FAI to Barrow is approximately 1.5 hours leaving about 5 hours for data collection. For some of the other sites, for example St. Lawrence Is. in the Bering Sea, the transit time is about 2 hours leaving only 4 hours for data collection.

**Table 4.1** NASA WFF P-3B instrumentation for the Arctic2003 campaign.

Sensor	Characteristics	Purpose	Sensor Scientist
Polarimetric Scanning Radiometer (PSR-A) (see Table 3.2)	Operating Frequencies (H&V-pol): 10, 18, 22, 37, 89 GHz	Simulate AMSR-E Measurements.	Dr. Gasiewski/NOAA/ETL
Polarimetric Scanning Radiometer (PSR-CX)	Operating Frequencies (H&V-pol): 6, 10 GHz	Simulate AMSR-E Measurements.	Dr. Gasiewski/NOAA/ETL
Turbulent Air Motion Measurement System (TAMMS)	Pressure ports coupled with pressure transducers, temperature sensors, and water vapor instruments.	Measure turbulent heat and moisture fluxes over coastal polynyas	Dr. K. Lee Thornhill/ NASA Langley Dr. John Barrick/NASA Langley
IR radiometer	9.6-11 $\mu\text{m}$ radiometer	Surface temperature	
Airborne Topographic Mapper (ATM-II)	Scanning Lidar altimeter combined with a differential GPS system	Maps ice surface topography at high resolution	William Krabill/NASA Wallops
Video and digital cameras	Tv video camera; 3 megapixel digital camera (KODAK)	Visible record of ice surface	William Krabill/NASA Wallops

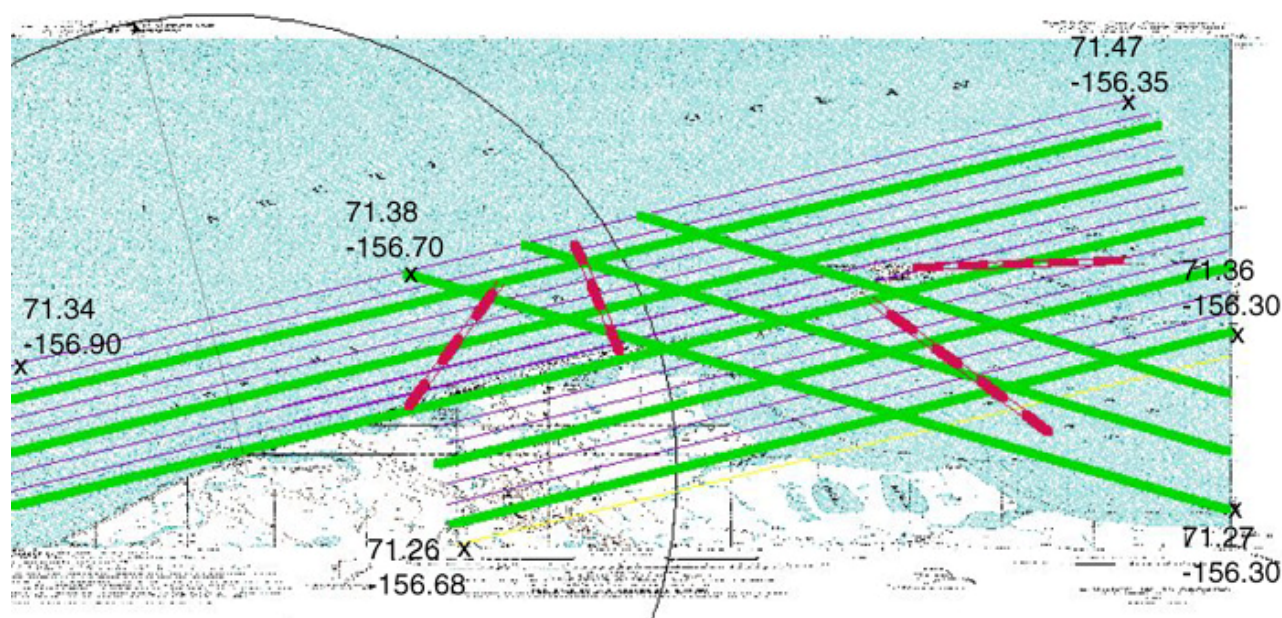


**Figure 4.3** Tentative flight lines for overflying the Barrow study area with the NASA P-3 aircraft.

**Table 4.2** P-3 Flight Objectives

FLIGHT NO.	OBJECTIVE	REGION	FLIGHT PATTERN / ALTITUDE	OPTIMAL WX AND SFC CONDITIONS
1	Compare P-3/AMSR-E ice concentrations in areas of new, young & first-year ice	St. Lawrence Is., Bering Sea	Hi-altitude mosaic (4,500 ft)	Clear wx; open polynya
1A	Measure sfc flux fall-off with ice conc. & type; compare computed sfc fluxes from AMSR-E & P-3	St. Lawrence Is., Bering Sea	Lo-altitude stack (500, 750, 1500 ft)	Clear wx; open polynya
2	Compare P3/AMSR-E sea ice concentrations in areas in the marginal ice zone & across the ice edge.	St. Lawrence Is., and the Bering Sea edge	Hi-altitude mosaic (21,000 ft)	Clear wx; open polynya
3	Compare P3/AMSR-E ice concentrations in areas of new, young & first-year sea ice	St. Lawrence Is., Bering Sea	Hi-altitude mosaic (4,500 ft)	Clear wx; open polynya
3A	Measure sfc flux fall-off with ice conc. & type; compare calculated sfc fluxes from AMSR-E & P-3	St. Lawrence Is., Bering Sea	Lo-altitude stack (500, 750, 1500 ft)	Clear wx; open polynya
4	Compare P3/AMSR-E ice concentrations in first-year & multiyear ice areas	Beaufort Sea	Hi-altitude mosaic (21,000 ft)	Clear wx; first-year/ multiyear ice type mix
4A	Compare P3/AMSR-E ice concentrations in first-year & multiyear ice areas	Beaufort Sea	Lo-altitude mosaic (4,500 ft)	Clear wx; first-year/ multiyear ice type mix
5	Compare P-3 snow depth & ice temperatures with sfc measurements	Barrow, AK	Lo-altitude transects (500 ft)	Clear wx
6	Compare P-3 snow depth & ice temperatures with sfc measurements	Barrow, AK	Lo-altitude transects (500 ft)	Clear wx
7	Compare P-3/AMSR-E ice concs. above/below clouds	Chukchi Sea	Hi-altitude mosaic (21,000 ft)	Clear/cloudy wx; range of ice conc.
7A	Compare P-3/AMSR-E ice concs. above/below clouds	Chukchi Sea	Lo-altitude mosaic (4,500 ft)	Clear/cloudy wx; range of ice conc.

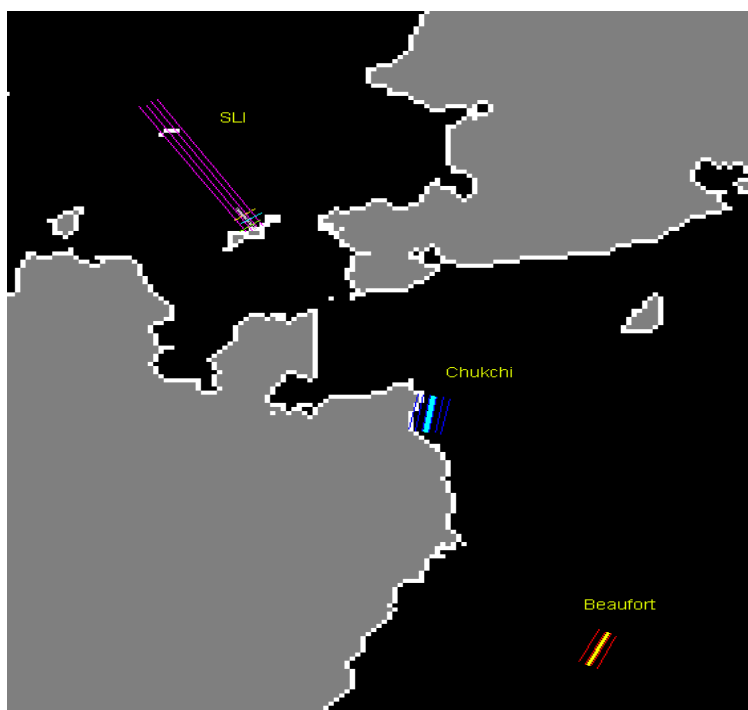


**Figure 4.4** Overview of the NASA P-3 flight lines for the Bering, Beaufort, and Chukchi seas.

Satellite/aircraft coordination is essential in meeting the objectives of this campaign. The swath of the EOS Aqua AMSR-E instrument (1445 km) is sufficiently wide to permit complete coverage daily over all areas to be flown with the P-3. The time of AMSR-E observations over these areas will be in early afternoon which coincides with the estimated 10 am to 2 pm time period of data collection for the P-3. The primary satellite sensors of interest are summarized in Table 4.3.

**Table 4.3** Summary of satellite sensors for the AMSR-E sea ice validation campaign.

Satellite	Sensor	Range of Operating Frequencies	Maximum Resolution
EOS Aqua	AMSR-E	7-89 GHz	5 km
EOS Aqua	MODIS	0.4-14.5 $\mu\text{m}$	250 m
ADEOS II	AMSR	7-89 GHz	4 km
Landsat 7	ETM+	.5-12.5 $\mu\text{m}$	15 m
DMSP F11-F15	SSMI	19-85 GHz	12 km
RADARSAT	SAR	5.3 GHz	8 m
ICESat	GLAS	1064 nm laser	70 m

Almost all of the flights are planned for clear weather conditions (Table 4.2). This will allow comparisons with those sensors that require cloud-free conditions to observe the surface such as MODIS, ETM+, and GLAS. Arrangements have been made for the acquisition of data by these sensors during each of the flights. The high resolution of these sensors permits them to be used for validating

the retrieved AMSR-E and PSR sea ice concentrations. While SAR does provide a high resolution capability, there are ambiguities in the interpretation of sea ice concentration arising from surface roughening of open water areas within the ice pack and at the ice edge by wind.

## **5 MODELING AND SENSITIVITY ANALYSES**

Radiative transfer modeling combines sea ice and atmospheric components to simulate top-of-the-atmosphere (TOA) brightness temperatures at AMSR-E frequencies. Our approach applies modeling in two ways. First, with the aid of the in situ data described above, we will calculate a synthetic AMSR-E data set that encompasses a wide range of surface and atmospheric conditions. Using these synthetic data as input to the AMSR-E algorithms, we will quantify the error statistics of the NT2, ABA, BBA, snow cover, and ice temperature retrievals as a function of local conditions. The second approach to be used is to validate the AMSR-E retrievals using forward modeling. In this approach, an ice and atmosphere "state" is defined. This state is then used to simulate TOA brightness temperatures. The simulated brightness temperatures are compared to the measured AMSR-E and/or P-3 PSR brightness temperatures. Discrepancies between the simulated and observed temperatures reflect errors in (a) the pre-defined state (the AMSR-E-derived ice concentrations, for example); (b) modeling errors; and (c) measurement errors (i.e., accuracy of the microwave radiometers). In addition, differences in sensor calibration will also be taken into account. For AMSR-E validation, we will be able to characterize the atmosphere reasonably well using UAV data and other Barrow observations, so we expect to be able to isolate the error associated with the algorithm-derived surface conditions. This method provides a direct way of quantifying product accuracies, and will allow us to identify algorithm shortcomings and thus suggest possible improvements.

The sea ice/atmospheric model to be used is that developed by Fuhrhop et al. (1997) called MWMOD, which we have applied previously for sensitivity studies (Stroeve et al., 1998). MWMOD computes brightness temperatures in the microwave frequency range for polar regions, including sea ice, open ocean and atmosphere, and has been applied by us previously for sensitivity studies (Stroeve et al., 1998). The Microwave Emission Model of Layered Snowpacks (MEMLS; Wiesmann and Metzler, 1999) will also be used to provide improved simulation of snowpack and multiyear ice. For applications of the models as a validation tool (via forward modeling of the AMSR-E-defined ice state), brightness temperatures for open water and ice can be prescribed, with the results compared to those achieved using the surface model. This will help alleviate the effects of inaccuracies in the surface modeling.

## **6 PROGRAM MANAGEMENT AND COORDINATION**

The overall management and coordination of the AMSR-E Team Validation Program will be the responsibility of Dr. Elena Lobl. This includes data set management and coordination among team members. The specific managerial responsibilities for the Arctic sea ice component of the validation effort is provided in Table 6.0. The responsibilities include the planning, coordination, execution of the task, data collection, and analysis. The data sets will be shared among investigators for intercomparison and analysis. The exchange of validation data sets between this program and Dr. Comiso's Antarctic program is essential. Exchanges of data will be undertaken as soon as final calibration and quality control are completed. This exchange of data sets will insure that all AMSR-E standard sea ice products will be validated for both Arctic and Antarctic.

An essential element of any field campaign is close coordination among field personnel. Coincident operations of the P-3 and Aerosondes (as well as any other aircraft in the area) will require development of flight plans and communications to assure safety. The study area is near the commercial airport at Barrow, so coordination with airport operations will be necessary. If possible, direct radio contact between the Aerosonde operators and the NASA P-3 during flight will be arranged for safety and also in case of delays, changes in flight plans, or other problems. It will also be necessary to have a communications plan to allow Barrow researchers and the P-3 operations to exchange information and coordinate flight times and plans prior to and subsequent to flights. This will be achieved via phone, fax, or internet.

Given the limited nature of the in situ data collection, every effort must be made to maximize the value of the data sets and assure that surface measurements are obtained at locations and times that best complement the aircraft and satellite observations. To help achieve this, we propose that the Barrow campaign begin with low altitude P-3, Aerosonde and field data collection. As soon as possible, these data should be processed in the field so that limited cross-checking of results, checking on navigation and coincident sampling can be assured. The effort will then continue with the remaining sampling plan for coverage of wider areas, but data should continue to be collected by all platforms over the selected areas. For example, the P-3 should plan on overflying the local Barrow area at some point during each Beaufort Sea flight. This should be feasible given the small area of the field site. As the campaign continues, initial near-Barrow data will be examined for areas with high gradients or otherwise noteworthy signals that can be used to plan more field sampling of any unusual areas or undersampled conditions. The Barrow-area campaign should end with the same low altitude acquisitions as at the beginning, to ensure sampling over the longest time period possible to capture the greatest temporal changes in the area of most field data. The combined surface, aircraft, satellite data collection effort will also require maximum use of tools to aid georeferencing among the different data sets. This is essential to maximize the value of the small study area, and is further discussed in Section 3.3.1.

**Table 6.1** Managerial responsibilities for the Arctic Sea Ice Validation Program

<b>TASK</b>	<b>RESPONSIBLE INVESTIGATORS</b>
NASA WWF P-3B Campaign	D. Cavalieri, A. Gasiewski, T. Markus, B. Walter
NSF Aerosonde UAV Campaign	J. Maslanik
Surface-Based Measurements	M. Sturm, J. Maslanik
Modeling and Sensitivity Studies	T. Markus, J. Stroeve, J. Heinrichs

## **7 DATA MANAGEMENT AND DATA AVAILABILITY**

Overall data management for the AMSR-E Validation Program will be the responsibility of Dr. Elena Lobl. Data management and availability for each subtask listed in Table 6.0 will be the responsibility of the corresponding investigators. Data sets will be made available and archived as soon as the data have been calibrated and quality controlled. It is anticipated that the data will be archived no later than one year after the field campaign is completed.

## 8 ARCTIC CAMPAIGN SCHEDULE

YEAR	02				03				04				05				06			
Task/Quarter	1	2	3	4	1	2	3	4	1	2	3	4	1	2	3	4	1	2	3	4
EOS Aqua Launch		X																		
1. Satellite intercomparisons																				→
2. Beaufort/Bering a/c flights					X															
3. P-3 aircraft data analysis											→									
4. Bering/Chukchi a/c flights												X								
5. P-3 aircraft data analysis																				→
6. Prelaunch Barrow UAV flights/in situ data analysis		X			X	→														

## 9 REFERENCES

Aagaard, K., L. K. Coachman, and E. C. Carmack, On the halocline of the Arctic Ocean, *Deep Sea Res.*, 29, 529-545, 1981.

Björk, G., A one-dimensional time-dependent model for the vertical stratification of the upper Arctic Ocean, *J. Phys. Oceanogr.*, 19, 52-67, 1989.

Brown, E., C. Friehe and D. Lenschow, The use of pressure fluctuations on the nose of an aircraft for measuring air motion. *J. Clim. Appl. Meteor.*, 22, 171-180, 1983.

Cavalieri, D. J., NASA Sea Ice Validation Program for the Defense Meteorological Satellite Program Special Sensor Microwave Imager, *J. Geophys. Res.*, 96, 21,969-21,970, 1991.

Cavalieri, D. J., A microwave technique for mapping thin sea ice, *J. Geophys. Res.*, 99, 12,561-12,572, 1994.

Cavalieri, D. J., The validation of geophysical parameters using multisensor data, Chapter 11 in *Microwave Remote Sensing of Sea Ice*, edited by F. D. Carsey, American Geophysical Union Monograph 68, 233-242, 1992.

Cavalieri, D. J., EOS Aqua Sea Ice Validation Program: Meltpond2000, NASA Technical Memorandum 2000-209972, National Aeronautics and Space Administration, Goddard Space Flight Center, Greenbelt, MD 20771, pp. 31, December 2000.

Cavalieri, D. and S. Martin, The Contribution of Alaskan, Siberian, and Canadian coastal polynyas to the cold halocline layer of the Arctic Ocean, *J. Geophys. Res.*, 99, 18343-18362, 1994.

Cavalieri, D. J., J. P. Crawford, M. R. Drinkwater, D. T. Eppler, L. D. Farmer, R. R. Jentz, and C. C. Wackerman, Aircraft active and passive-microwave validation of sea ice concentration from the DMSP SSM/I, *J. Geophys. Res.* **96**, 21,989-22,008, 1991.

Cavalieri, D. J., P. Gloersen, and T. T. Wilheit, Aircraft and satellite passive-microwave observations of the Bering Sea ice cover during MIZEX West, *IEEE Trans. Geoscience and Remote Sensing*, **GE-24**, 368-377, 1986.

Comiso, J. C. and C. W. Sullivan, Satellite microwave and in situ observations of the Weddell Sea Ice Cover and its Marginal Ice Zone, *J. Geophys. Res.*, 91(C8), 9663-9681, 1986.

Comiso, J.C., D. Cavalieri, C. Parkinson, and P. Gloersen, Passive microwave algorithms for sea ice concentrations, *Remote Sensing of the Env.*, 60(3), 357-384, 1997.

Comiso, J.C., D. J. Cavalieri, and T. Markus, Sea ice concentration, ice temperature, and snow depth using AMSR-E data, *IEEE Trans. Geoscience and Remote Sensing*, in press, 2003.

J. C. Comiso, and H.J. Zwally, Temperature Corrected Bootstrap Algorithm, *IEEE IGARSS'97 Digest*, Vol. 3, pp. 857-861, 1997.

Fuhrhop, R., C. Simmer, M. Schrader, G. Heygster, K-P. Johnsen, P. Schussel, *Study of Passive Remote Sensing of the Atmosphere and the Surface Ice: Executive Summary and Final Report*, ESA ESTEC Contract No.11198/94/NL/CN, Berichte IfM Kiel, Nr. 29, 1997.

Gawarkiewicz, G., and D. C. Chapman, A numerical study of dense water formation and transport on a shallow, sloping continental shelf, *J. Geophys. Res.*, 100, 4489-4507, 1995.

Gloersen, P., W. J. Campbell, D. J. Cavalieri, J. C. Comiso, C. L. Parkinson, H. J. Zwally, Arctic and Antarctic Sea Ice, 1978-1987: Satellite Passive Microwave Observations and Analysis, National Aeronautics and Space Administration, Special Publication 511, Washington, D.C., pp.290, 1992.

Grenfell, T.C., J.C. Comiso, M.A. Lange, H. Eicken, and M.R. Wenshahan, Passive microwave observations of the Weddell Sea during austral winter and early spring, *J. Geophys. Res.*, 99(C5), 9995-10,010, 1994.

Holland, G. J., T. McGeer and H. Youngren, Autonomous Aerosondes for economical atmospheric soundings anywhere on the globe. *Bull. Amer. Met. Soc.*, 73, 1987-1998, 1992.

Holland, G. J., P. J. Webster, J. A. Curry, G. Tyrell, D. Gauntlett, G. Brett, J. Becker, R. Hoag, and W. Vaglianti, The Aerosonde robotic aircraft: A new paradigm for environmental observations. *Bull. Amer. Met. Soc.*, 82 (5), 889-901, 2001.

Holmgren, J., M. Sturm, N. E. Yankielun, and G. Koh, Extensive measurements of snow depth using FM-CW radar. *Cold Regions Sci. & Tech.* **27**, 17-30, 1998.

Jezek, K. C., D. K. Perovich, K. M. Golden, C. Luther, D. G. Barber, P. Gogineni, T. C. Grenfell, A. K. Jordan, C. D. Mobley, S. V. Nghiem, and R. G. Onstott, A broad spectral, interdisciplinary investigation

of the electromagnetic properties of sea ice, *IEEE Trans. Geosci. and Remote Sensing*, Vol.36, No.5, 1633-1641, 1998.

Markus, T. and D. J. Cavalieri, Snow depth distribution over sea ice in the Southern Ocean from satellite passive microwave data, *Antarctic Sea Ice: Physical Processes, Interactions and Variability*, Antarctic Research Series, Volume 74, pp 19-39, American Geophysical Union, Washington, DC, 1998.

Markus, T. and D. J. Cavalieri, An enhanced NASA Team sea ice algorithm, *IEEE Trans. Geosci. and Remote Sensing*, 38, 1387-1398, 2000.

Markus, T., D.J. Cavalieri, and A. Ivanoff, The potential of using Landsat 7 ETM+ for the classification of sea ice surface conditions during summer, *Ann. Glaciol.*, in press, 2001.

Martin, S., B. Holt, D. J. Cavalieri, and V. Squire, Shuttle Imaging Radar B (SIR-B) Weddell Sea ice observations: A comparison of SIR-B and Scanning Multichannel Microwave Radiometer ice concentrations, *J. Geophys. Res.* **92**, 7173-7179, 1987.

Maykut, G. A., Energy exchange over young sea ice in the central Arctic, *J. Geophys. Res.*, 83, 3646-3658, 1978.

National Snow and Ice Data Center(NSIDC), NSIDC, DMSP SSM/I Brightness Temperatures and Sea Ice Concentration Grids for the Polar Regions on CD-ROM User's Guide, *National Snow and Ice Data Center, Special Report - 1*, Cooperative Institute for Research in Environmental Sciences, University of Colorado, Boulder, CO, January 1996.

Steffen, K. and J. A. Maslanik, Comparison of Nimbus 7 Scanning Multichannel Microwave Radiometer radiance and derived sea ice concentrations with Landsat imagery for the North Water area of Baffin Bay, *J. Geophys. Res.*, 93, 10,769-10,781, 1988.

Steffen, K. and A. Schweiger, NASA Team algorithm for sea ice concentration retrieval from Defense Meteorological Satellite Program Special Sensor Microwave Imager: comparison with Landsat satellite imagery, *J. Geophys. Res.*, 96, 21971-21987, 1991.

Steffen, K., D. J. Cavalieri, J. C. Comiso, K. St. Germain, P. Gloersen, J. Key, I. Rubinstein, D. Thomas, Passive microwave algorithms, Chapter 10 in Microwave Remote Sensing of Sea Ice, American Geophysical Union Monograph 68, edited by F. D. Carsey, 201-231, 1992.

Stroeve, J., J. Maslanik, and X. Li, An Intercomparison of DMSP F11- and F13-derived Sea Ice Products, *Remote Sensing of the Environment*, Vol. 64, 132-152, 1998.

Sturm, M., K. Morris, and R. Massom, The winter snow cover of the west Antarctic pack ice: its spatial and temporal variability. In *Antarctic Sea Ice: Physical Processes, Interactions and Variability*, M. Jeffries, ed., *Ant. Res. Series*, **74**, 1-18, 1998.

Sturm, M., J. Holmgren, and D. Perovich, In review, *The winter snow cover on the sea ice of the Arctic Ocean at SHEBA: Temporal evolution and spatial variability*. *Journal of Geophysical Research-Oceans*

Weingartner, T. J., D. J. Cavalieri, K. Aagard, and Y. Sasaki, Circulation, dense water formation, and outflow on the northeast Chukchi shelf, *J. Geophys. Res.*, 103, 7647-7661, 1998.

Winsor, P., and G. Björk, Polynya activity in the Arctic Ocean from 1958 to 1997, *J. Geophys. Res.*, 105, 8789-8803, 2000.

Walter, B., A Study of the Planetary Boundary Layer over the Polynya Downwind of St. Lawrence Island in the Bering Sea using Aircraft Data, *Bound-Layer Meteor.*, 48, 255-282, 1989.

Wiesmann, A. and C. Metzler, Microwave Emission Model of Layered Snowpacks, *Remote Sens. Environ.*, 70, 307-316, 1999.